Surface properties and catalytic activity of ferrospinels of nickel, cobalt and copper, prepared by soft chemical methods

C.G. Ramankutty, S. Sugunan*

Department of Applied Chemistry, Cochin University of Science and Technology, Kochi 22, Kerala, India

Abstract

Ferrospinels of nickel, cobalt and copper and their sulphated analogues were prepared by the room temperature coprecipitation route to yield samples with high surface areas. The intrinsic acidity among the ferrites was found to decrease in the order: cobalt > nickel > copper. Sulphation caused an increase in the number of weak and medium strong acid sites, whereas the strong acid sites were left unaffected. Electron donor studies revealed that copper ferrite has both the highest proportion of strong sites and the lowest proportion of weak basic sites. All the ferrite samples proved to be good catalysts for the benzoylation of toluene with benzoyl chloride, copper and cobalt ferrites being much more active than nickel ferrite. The catalytic activity for benzoylation was not much influenced by sulphation, but it increased remarkably with calcination temperature of the catalyst. Surface Lewis acid sites, provided by the octahedral cations on the spinel surface, are suggested to be responsible for the catalytic activity for the benzoylation reaction. © 2001 Elsevier Science B.V. All rights reserved.

Keywords: Spinel ferrites; Ferrospinels; Friedel–Crafts benzoylation of toluene; Sulphated ferrospinels; Spinels by 'soft' chemical methods

1. Introduction

Historically, spinel ferrites of formula $A^{II}Fe_2^{III}O_4$ have attracted the attention of physicists and technologists since these are magnetic semiconductors, suitable for use in microwave devices [1]. At the same time, these have well-established catalytic properties for many reactions such as oxidative dehydrogenation of hydrocarbons, decomposition of alcohols, selective oxidation of carbon monoxide, decomposition of hydrogen peroxide, and hydrodesulphurisation of petroleum crude. The catalytic properties of ferrospinels crucially depend on the distribution of cations among the octahedral and tetrahedral sites of the spinel structure. Jacobs et al. [2] established

that, in spinels, the octahedral sites are almost exclusively exposed in the crystallites and that the catalytic activity was mainly due to octahedral cations.

The usual ceramic method of preparing ferrospinels gives inhomogeneous and aggregate particles with low surface areas. The recently developed low temperature coprecipitation method [3] yields homogeneous and fine ferrite powders with high surface areas and catalytic activity. Such samples were found to be effective catalysts for alkylation of aniline [4] and phenol [5]. The present investigation is devoted to the study of the surface properties and catalytic activity of the ferrospinels of nickel, cobalt and copper, prepared by the low temperature coprecipitation route. The surface properties have been evaluated by adopting various physico-chemical methods. The catalytic activity is studied for the liquid phase Friedel–Crafts benzoylation of toluene.

* Corresponding author. Fax: +91-484-532495.
E-mail address: ssg@cusat.ac.in (S. Sugunan).

It is well established that surface modification of metal oxides with sulphate ions enhances their acidities and, in some cases, makes them superacidic. Since sulphated ferric oxide shows superacidic properties [6], we have taken up, as an interesting extension of our work, the study of sulphate modification of these ferrospinels. Our literature survey reveals that sulphation studies of spinel-type mixed oxides have not been reported so far. Our investigations revealed that these spinel ferrites are remarkably active for the benzoylation of toluene and that sulphation, although it enhanced the acidities of the samples, did not influence much with the catalytic activities for benzoylation. Cobalt ferrite was the most active sample at the activation temperature of 300°C, while copper ferrite was the most active one at the activation temperature of 500°C.

2. Experimental

2.1. Synthesis

Metals were coprecipitated as their hydroxides from a stoichiometric mixture of 2.6 M solution ferric nitrate and 3.4 M solution of other nitrates, using 5.3 M sodium hydroxide as the precipitating alkali. The temperature of the slurry rose to about 45°C due to the exothermic nature of the precipitation reaction. The pH of the final slurry was carefully adjusted to 10. The precipitate was kept overnight for ageing and washed free of nitrate ion and alkali. It was then filtered, dried at 120°C for 48 h and calcined at 300°C for 3 h to achieve transformation into spinel phase. The dried materials were powdered and sieved below 75 μm mesh.

Sulphation was done by the standard 'impregnation' method by agitating the spinel oxide samples immersed in 0.2 M ammonium sulphate solution for 4 h. The mixture was kept overnight and filtered without washing. It was then dried at 120°C for 24 h, powdered and sieved below 75 μm mesh.

2.2. Characterisation

2.2.1. Physical methods

The catalyst samples were characterised by adopting various physical methods such as XRD

analysis, infrared spectra, BET surface area, pore volume measurements, Energy dispersive X-ray (EDX) analysis, thermogravimetric analysis (TGA) and Mossbauer spectra. The samples which had been activated for 3 h at temperatures of 300 or 500°C were studied.

The X-ray powder diffactometer traces were taken using RIGAKU D/MAX-C instrument with Cu Kα radiation. The FTIR spectra were taken using Shimadzu FTIR-8101 and the DRIFT spectra were taken using Shimadzu DR-IR. The BET surface area was measured by nitrogen adsorption at liquid nitrogen temperature using a Micromeritics Gemini Analyser. The pore volumes were determined using a Quantachrome mercury porosimeter. Quantitative elemental analysis of the samples was done by EDX fluorescence analysis (Stereoscan 440 Cambridge, UK). The Mossbauer spectra were taken using Austin (USA) S-600 spectrometer. The TGA has been done using TGA-50 (Shimadzu) at the rate of heating of 10°C/min.

2.2.2. Surface properties — acidity/basicity

2.2.2.1. Surface electron donating properties (evaluation of Lewis basicity).
Investigation of the strength and distribution of electron donor (ED) sites on oxide surfaces using electron acceptors (EA) having different electron affinity values has been a well-established technique. The electron acceptors used in the study were 7,7,8,8-tetracyanoquinodimethane (TCNQ), 2,3,5,6-tetrachloro-p-benzoquinone (chloranil) and p-dinitrobenzene (PDNB) with electron affinity values of 2.84, 2.40 and 1.77 eV, respectively. TCNQ (Merck-Schuchandt), chloranil (Sisco Research Laboratories Pvt., Ltd.) and PDNB (Koch Light Laboratories, Ltd.) were purified by recrystallisation from acetonitrile, benzene and chloroform, respectively. Acetonitrile (Qualigens Fine Chemicals) was used as solvent. It was purified by drying over silica gel (60–120 mesh size) activated at 110°C for 2 h, followed by distillation with anhydrous phosphorus pentoxide, the fraction distilling between 80 and 82°C being collected.

Adsorption study was carried out over 0.5 g of the activated catalyst placed in a cylindrical glass vessel fitted with an airtight stirrer. 10 ml of a solution of EA in acetonitrile was then admitted to the catalyst. Stirring was continued for 4 h at room temperature. The amount of EA adsorbed was determined from the

difference in concentration of EA in solution before and after adsorption, which was measured using a Shimadzu UV–VIS spectrophotometer (λ_{max} of EA in acetonitrile $= 393.5$ nm for TCNQ, 288 nm for chloranil and 262 nm for PDNB).

2.2.2.2. Evaluation of surface acidity — gravimetric adsorption of n-butylamine followed by TGA. Gravimetric adsorption of n-butylamine followed by TGA is a very simple method for determining the strength and distribution of acid sites on catalyst surfaces [7,8]. Catalyst samples were kept in a desiccator saturated with n-butylamine vapour at room temperature for 48 h. Then the weight loss of the adsorbed sample was measured by TGA (Shimadzu TGA-50) operating between 40 and 600°C at the rate of 20°C/min. The weight losses between 150 and 300, 301 and 450, and 451 and 600°C were considered to be measures of weak, medium and strong acid sites, respectively.

2.2.3. Liquid phase benzoylation reaction of toluene

Toluene (Qualigens Fine Chemicals) was purified by the standard procedure [9] and benzoyl chloride from Merck was used as such. A mixture of toluene and benzoyl chloride in the molar ratio 3.6:1 was refluxed in an oil bath at the boiling point of the mixture with 0.100 g of the activated catalyst sample for 30 min. The product was analysed by gas chromatography (Chemito 8510, SE 30 column, FID detector, nitrogen as carrier gas, injection port temperature 250°C, column temperature-programmed as 100°C for 2 min followed by heating at the rate of 7°C/min upto 170°C, detector temperature 250°C). The products were identified by GC-MS.

3. Results and discussion

3.1. Characterisation by physical methods

3.1.1. XRD analysis

The experimental XRD data of these ferrite samples agreed very closely with the standard values given in the JCPDS Data Cards, thus confirming the spinel phase and the inverse spinel structure. A typical XRD pattern is given in Fig. 1. As the temperature of calcination increases, the XRD peaks become sharper as a result of shift towards greater crystallinity.
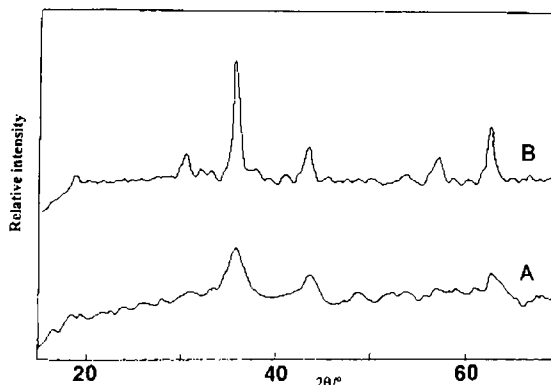

Fig. 1. XRD patterns of NiFe₂O₄. (A) Calcined at 300°C and (B) 500°C.

The XRD patterns of all the samples, including the sulphate-modified ones, were found to be very much alike. This is expected because all the ferrite samples have the same inverse spinel structure and the elements responsible for the compositional differences viz. nickel, cobalt and copper have close atomic numbers and hence close atomic scattering factors for X-rays. EDX results showed that sulphate-loading was about 1% by mass of sulphur in the modified samples. This is an insufficient amount to cause changes in the XRD patterns [10]. The average particle diameter of each sample has been calculated using the Scherrer equation [11]; the value ranged between 16 and 26 nm, proving the fine nature of the powders.

3.1.2. Infrared spectra

The DRIFT spectra, taken in 400–1000 cm^{-1} region, typically showed two strong bands ν_1 and ν_2 around 700 and 500 cm^{-1}, respectively. Waldron [12] showed that two absorption bands below 1000 cm^{-1} were a common feature of all ferrites and assigned the high frequency band to the tetrahedral M–O stretching and the low frequency band to the octahedral M–O stretching vibrations. Sulphate-loading has been qualitatively confirmed from the infrared spectra, which always showed additional bands in the range 1200–1000 cm^{-1} for the sulphated samples. These bands consisted of four absorptions — two strong ones near 1100 and 1050 cm^{-1} and two weak ones near 1150 and 990 cm^{-1}, which sometimes appeared only as shoulders. Figs. 2 and 3 show typical DRIFT and FTIR spectra for nickel ferrite samples.

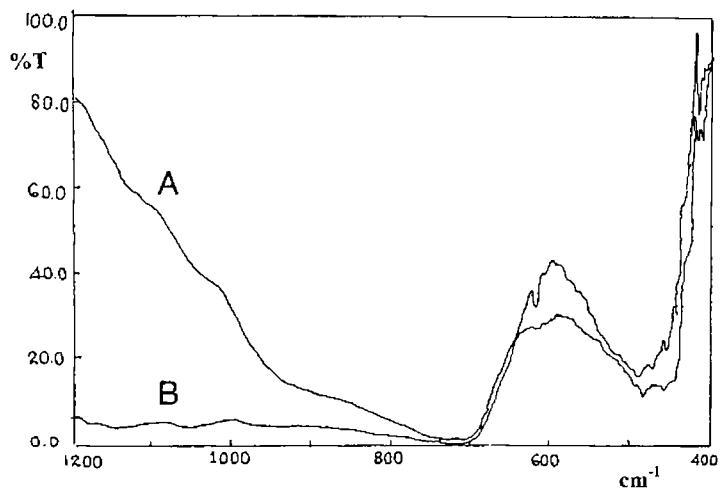Fig. 2. DRIFT spectra of ferrites. (A) NiFe$_2$O$_4$ and (B) sulphated NiFe$_2$O$_4$, both calcined at 300°C.

Infrared spectra of sulphated metal oxides, especially the superacidic ones, have been the subject of detailed studies for explaining the cause of superacidity and for proposing structure models for the surface sulphate species [13–17]. A common feature of all superacidic sulphated oxides is the presence of a strong band near 1400 cm^{-1} and a number of bands in the range 1150–1000 cm^{-1} [15]. The strong band near 1400 cm^{-1}, representing the asymmetric stretching frequency of S=O, is often regarded as the characteristic band of sulphate-promoted superacids [18,19]. The presence of this band, and hence the
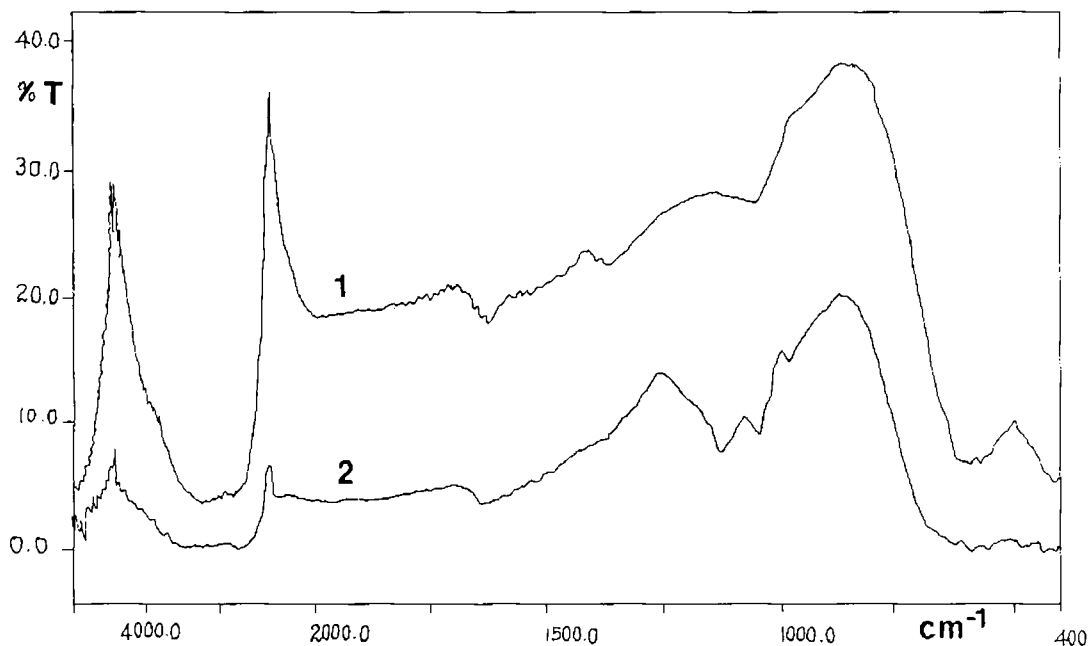

Fig. 3. FT-IR spectra of ferrites. (1) NiFe$_2$O$_4$ and (2) sulphated NiFe$_2$O$_4$, both calcined at 300°C.

43

superacidity, depend very critically on the water con-
tent of the sulphated oxides. This band, present in a
high dehydration stage, will gradually disappear with
hydration of the sample, leaving only the low fre-
quency bands in the IR spectra [20]. Returning to the
present case, lack of a strong band near 1400 cm^{-1}
suggests lack of superacidity in the sulphated spinel
samples. This is explained by the fact that many of the
characterisation and catalytic studies of the systems
were done at the activation temperature of 300°C,
at which the samples were still sufficiently hydrated.
This is evidenced by the broad XRD peaks at 300°C
(Fig. 1) and the TG results, which showed that dehy-
dration of the sulphated samples occurred just above
300°C. The IR bands obtained in the 1200-1000 cm^{-1}
region are typical of sulphato complexes in a biden-
tate configuration with C_{2v} symmetry [21] or of the
hydrogenosulphate-modified species, as suggested
for sulphated alumina or titania in the presence of
water [13]. The latter model is more appropriate to
the present case, as it can account for the increased
Bronsted acidity shown by the sulphated samples.

3.1.3. BET surface area, pore volume measurements, EDX and TGA

As expected, the surface areas (Table 1) increase
with sulphation (except for copper ferrite at 300°C)
and decrease with calcination temperature. Sulphation
inhibits sintering and delays the transition from amor-
phous to crystalline phase [17]. Copper ferrite shows
a drastic decrease in surface area with calcination.
The decrease in surface area with calcination is due to
the completion of dehydration concomitant with the
completion of crystallisation and growth of crystallite
size by sintering. Mercury porosimetry data on the

spinel samples show that both pore volume and pore
size decrease with sulphation, while, on calcination,
pore volume decreases but pore size increases. The
compositions of the spinel samples were checked by
EDX analysis and there was good agreement between
the experimental and theoretical values (Table 1). The
thermal stability of the samples were checked and
proved by TG and by the corresponding derivative
curves (DTG), which were almost horizontal from
about 400 to 700°C. The weight loss due to dehy-
dration occurred below 300°C for the unmodified
samples, but just above 300°C for the sulphated ones,
supporting the conclusion that sulphation delayed
transformation from amorphous to crystalline phase.
A new weight loss developed for the sulphated sam-
ples above 700°C; this should be due to the loss of
sulphate.

3.1.4. Mossbauer spectra

The Mossbauer parameters given in Table 1 give
information on the oxidation state, electronic environ-
ment and magnetic properties of the iron nuclei in the
ferrite samples and also on the particle size of these
samples. The characteristic Mossbauer isomer shift
(IS) for Fe^{3+} with the total spin, $S = 5/2$, is within
0.2-0.5 mm/s with respect to natural iron [22]. The IS
values of Fe^{3+} in the tetrahedral (T) and octahedral
(O) sites are very close so that the peaks overlap, giv-
ing a single IS value for the iron in the ferrite samples.
It is evident from the IS data of Table 1 that all the
iron atoms in these ferrite samples are in the +3 oxi-
dation state. The Mossbauer spectra given in Fig. 4a
and b are best fitted by doublets and thus show para-
magnetic quadruple patterns. The spectrum of cobalt
ferrite (Fig. 4c) is distinct and is typical of a sample

Table 1
Characterisation of the ferrospinels by physical methods

System	Mass% by EDX[a]	Mossbauer parameters[b] (±0.02 mm/s)			BET surface area (m^2/g)[c]	
		IS	ΔE_Q	Line width	300°C	500°C[d]
NiFe$_2$O$_4$	Ni: 32.2 (34.4), Fe: 67.8 (65.6)	0.34	0.60	0.58	152.8 (196.3)	45.1 (77.9)
CoFe$_2$O$_4$	Co: 34.2 (34.5), Fe: 65.8 (65.5)	–	–	–	94.6 (107.4)	32.2 (46.3)
CuFe$_2$O$_4$	Cu: 35.2 (36.3), Fe: 64.8 (63.7)	0.34	0.74	0.56	187.9 (187.7)	19.8 (32.5)

[a] Theoretical mass% in parentheses.
[b] Data with respect to natural iron as source.
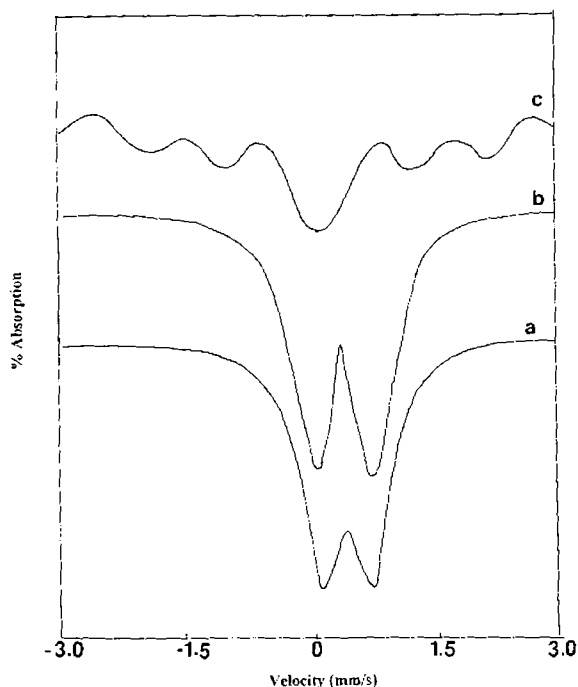[c] Surface area of sulphated samples in parentheses.
[d] Activation temperature.

Fig. 4. Room temperature Mossbauer spectra of spinel ferrites calcined at 300°C. (a) NiFe₂O₄; (b) CuFe₂O₄, and (c) CoFe₂O₄.

having superparamagnetic behaviour, a stage between paramagnetic and ferrimagnetic nature. Its Mossbauer parameters are not computed. The quadrupolar doublets prove the existence of an electric field gradient (EFG) about the iron nuclei, which interacts with the electric quadrupole moment of the iron nuclei in the excited state. Since Fe^{3+} has a half-filled 3d shell, the EFG arises only from the neighbouring ions and thus exists only at those sites having non-cubic symmetry. In the inverse spinel systems presently studied, the T-sites have no chemical disorder and thus experience no EFG. But the O-sites develop an EFG along the [1 1 1] zone direction, not only due to the chemical disorder from the surrounding metal cations but also from the oxygen ions. This is because the metal ion in the small T-site pushes the four surrounding oxygen anions in the [1 1 1] directions. The cubic symmetry (T_d) of the T-site is maintained, but the cubic symmetry (O_h) of the O-site is distorted and changes to trigonal (D_{3d}) symmetry, changing the trigonal component of the EFG [23]. The quadrupolar coupling constant (ΔE_Q), which is a measure of the magnitude

of EFG, is the largest for copper ferrite because of an additional distortion of charge symmetry here, caused by the Jahn–Teller effect.

It is well known that the ferrospinels of cobalt, nickel and copper are ferrimagnetic. However, the magnetic hyperfine splitting is missing in the spectra given in Fig. 4. This is because the particle size in these samples is not large enough to show ferrimagnetic effects. As the grain size becomes smaller, the magnetisation direction of each particle of the ultra-fine ferrite powder fluctuates by virtue of thermal energy (kT) and hence cannot be fixed as in large crystals, thus providing an average magnetisation of zero [24]. For cobalt ferrite (Fig. 4c), there is an emergence of a magnetic hyperfine pattern. This may be due to the sample being partially paramagnetic and partially ferrimagnetic simultaneously, as some particles are too small to maintain ferrimagnetic property while others are large enough to become ferrimagnetic.

3.2. Surface properties — acidity/basicity

3.2.1. Surface electron donating properties (evaluation of Lewis basicity)

To investigate the strength and distribution of electron donor (ED) sites on the oxide surface, adsorption experiments were performed using electron acceptors (EA) of varying electron affinity values, in acetonitrile solution. The adsorption was found to be of the Langmuir type. The limiting amounts have been estimated from the Langmuir plots (Figs. 5 and 6). The limiting amounts of TCNQ and chloranil adsorbed on the various catalytic systems are given in Table 2. The adsorption of PDNB was so negligible that the amount adsorbed was hard to estimate. Again, the adsorption of chloranil on all the samples and that of TCNQ on the sulphated samples were too low to be measured accurately at the activation temperature of 500°C. The data of Table 2 show that the limiting amount of EA adsorbed is higher for TCNQ than for chloranil. Since TCNQ is a strong electron acceptor, it forms anion radicals on both strong and weak donor sites. In other words, the limiting amount of TCNQ adsorbed gives a measure of strong as well as weak donor sites on the catalyst surface. But chloranil can accept electrons from strong and moderately strong donor sites only. Negligible adsorption of PDNB indicates absence of very strong electron donor sites in all
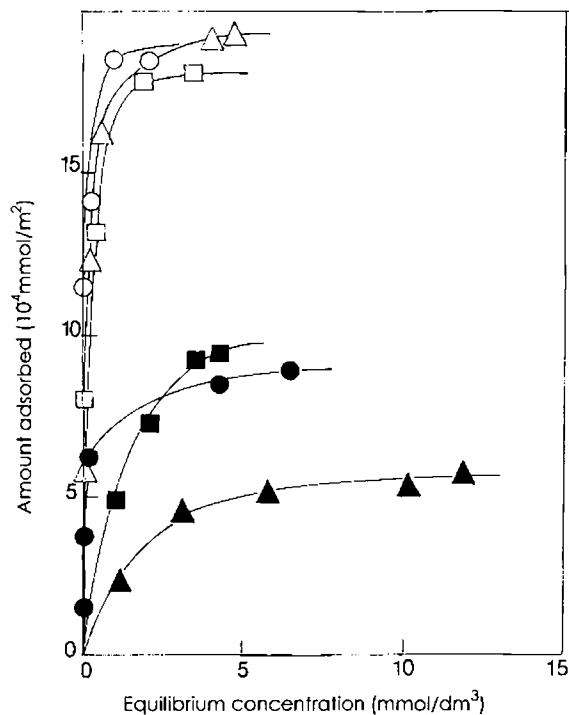
Fig. 5. Adsorption isotherms of TCNQ in acetonitrile over unmodified and sulphate-modified ferrites activated at 300°C. (O) NiFe₂O₄; (△) CoFe₂O₄; (□) CuFe₂O₄; (●) SO₄²⁻/NiFe₂O₄; (▲) SO₄²⁻/CoFe₂O₄; (■) SO₄²⁻/CuFe₂O₄.

Fig. 6. Adsorption isotherms of chloranil in acetonitrile over unmodified and sulphate-modified ferrites activated at 300°C. (O) NiFe₂O₄; (△) CoFe₂O₄; (□) CuFe₂O₄; (●) SO₄²⁻/NiFe₂O₄; (▲) SO₄²⁻/CoFe₂O₄; (■) SO₄²⁻/CuFe₂O₄.

systems. Electron donor strength of a metal oxide can be expressed as the limiting electron affinity value at which free anion radical formation, i.e. adsorption of the EA, is not observed at the metal oxide surface [25]. This suggests that adsorption sites on the ferrospinel systems act as electron donors to the EA molecule with electron affinity values less than 2.40 eV but greater than 1.77 eV. Accordingly, the limit of
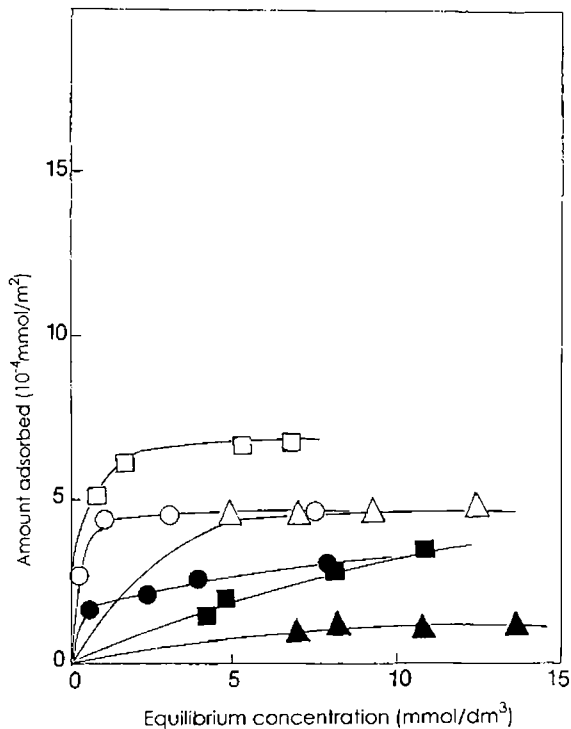
electron transfer from ED sites of ferrospinels to the EA molecule is located between 2.40 and 1.77 eV.

The difference between the limiting amounts of TCNQ and chloranil adsorbed gives an idea of the number of weak donor sites. From the data of Table 2, the distribution of strength and order of basicity of the ferrites follow as copper > cobalt ≅ nickel, regarding the strong and moderately strong basic sites

Table 2
Limiting amounts of the electron acceptors (EA) adsorbed over the ferrospinel systems

System	Limiting amount of EA adsorbed $(10^{-4} \text{ mmol/m}^2)^a$			
	$TCNQ^b$	$Chloranil^b$	$(TCNQ\text{-}Chloranil)^b$	$TCNQ^c$
NiFe₂O₄	18.3 (8.9)	4.4 (3.0)	13.9 (5.9)	29.9
CoFe₂O₄	19.0 (5.7)	4.6 (1.0)	14.4 (4.7)	28.6
CuFe₂O₄	18.0 (9.3)	6.7 (3 4)	11.3 (5.9)	40.4

[a] Limiting amounts adsorbed over the sulphated samples in parentheses.
[b] Activation temperature of 300°C.
[c] Activation temperature of 500°C.

and as cobalt $\cong$ nickel > copper, regarding the weak basic sites. Thus, copper ferrite has both the highest proportion of strong and the lowest proportion of weak basic sites. Sulphation reduces both the strong and weak basic sites in the ferrites almost evenly. Being acidic, sulphating agents preferentially attack at the basic sites, converting these to acidic sites. The intrinsic basicities are higher at higher activation temperature, as is evident from the limiting amount values of TCNQ adsorbed at 500°C.

Ferrospinels have both Lewis and Bronsted acid sites and Lewis basic sites. Electron donor sites come from electrons trapped in intrinsic defects or from surface hydroxyl groups [26] or from coordinatively unsaturated oxide ion associated with a neighbouring hydroxyl group [27]. At the calcination temperature of 300°C, the basic sites are mainly due to surface hydroxyl groups. The surface hydroxyl groups on a given catalyst can vary in their electron donating properties and this amounts to distribution of basic strengths [26].

It will be interesting to analyse, in this context, the order of acidity/basicity among the octahedral cations of these ferrospinels on the basis of the usual theoretical parameters like charge to radius ratio or electronegativity of the cations. From the crystal radii given by Shannon [28], the charge to radius ratios of the cations have been calculated; these vary as $Fe^{3+} \gg Ni^{2+} > Cu^{2+} \cong Co^{2+}$. It is generally accepted that a higher charge to radius ratio of the metallic ion gives a more acidic oxide. Thus, the acidity of the oxides is expected to vary in the above order and the basicity in the reverse order. We can also expect that the acidity of a metal ion will be directly proportional to the electronegativity of the metal cation. Using Sanderson's method [29], the electronegativity values of the metal ions have been computed; these vary as

$Fe^{3+} \gg Cu^{2+} > Ni^{2+} \cong Co^{2+}$. So the acidity varies in this order and the basicity in the reverse order. Thus, by the theoretical arguments, Fe^{3+} is the most acidic (least basic) ion while the order of acidity/basicity among the Cu^{2+}, Co^{2+} and Ni^{2+} ions does not always correlate. This is due to the fact that the acido-basic properties of these ions are close to one another and that the mixed oxide systems need not show the same trends of acidity/basicity as the single oxides.

For samples activated at 500°C, the basicity shows an increase. This is due to the creation of new electron donor sites at the higher temperature. Ferrospinels are generally n-type semiconductors which lose lattice oxygen on heating, causing anionic vacancies. The released electrons are accommodated by conversion of Fe^{3+} to Fe^{2+} ions and, in the case of copper ferrite, by conversion of Cu^{2+} to Cu^+ or even Cu. The presence of free electrons in defect sites causes an increased basicity and this increase is found to be the highest for copper ferrite. This can be due to the higher susceptibility of copper ferrite to the creation of defect sites with calcination, imposed by the higher thermal instability [30] and the special coordination described as (4 + 2) coordination [31] of copper(II) oxide.

3.2.2. Gravimetric adsorption of n-butylamine followed by TGA

The samples, after being kept in n-butylamine atmosphere at room temperature for 48 h, were subjected to TGA. The percentage weight losses per unit surface area were computed in three temperature ranges viz. 150–300, 301–450 and 451–600°C which were considered to be measures of weak, medium and strong acid sites, respectively. These data (Table 3) show that the total intrinsic acidity of the ferrites varies in the order: cobalt > nickel > copper, whereas the sulphated

Table 3

Data on acidity measurement of the ferrites by gravimetric adsorption of n-butylamine, followed by TGA

Systems (activated at 300°C)	% Weight loss (10^{-2} m^{-2})			
	Weak (150–300°C)	Medium (300–450°C)	Strong (450–600°C)	Total (150–600°C)
NiFe$_2$O$_4$	3.09	1.33	0.66	5.08
CoFe$_2$O$_4$	2.58	1.40	1.15	5.13
CuFe$_2$O$_4$	3.25	0.63	0.40	4.23
SO$_4{}^{2-}$/NiFe$_2$O$_4$	2.46	1.92	0.55	4.93
SO$_4{}^{2-}$/CoFe$_2$O$_4$	6.08	2.54	0.87	9.50
SO$_4{}^{2-}$/CuFe$_2$O$_4$	4.80	2.22	0.38	7.40

analogues show the order cobalt > copper > nickel. Sulphation creates an increase in the number of medium strong acid sites in all cases and also an increase in weak sites, except for nickel ferrite. The number of strong acid sites is a maximum for cobalt ferrite. Sulphation shows little influence on the number of strong acid sites.

Transition metal oxides are primarily redox catalysts and their acido-basic properties are only of secondary importance. Hence, less work has been done on investigating the acid–base properties of transition metal oxides. Although both acidic and basic sites exist on transition metal oxides, these are generally classed as acidic oxides or A-type oxides, as described by Auroux and Gervasini [32]. For a mixed oxide like ferrospinel, the acido-basic properties can be very decisive in determining their catalytic activities. Usually the weak and medium strong acid sites have a high proportion of Bronsted sites, while the strong acid sites are mainly of the Lewis-type [33]. If one puts the data of Tables 2 and 3 together, it is evident that a fair amount of reciprocality exists in the number of acid and basic sites of corresponding strengths among the catalyst samples. By reciprocality, we mean that, when the number of acid sites increases, the number of basic sites of corresponding strength decreases.

For catalyst technology, the most sensitive probe of catalyst performance will continue to be the rate and selectivity of a chemical reaction. We have tested the catalyst performance of these samples for benzoylation of toluene.

3.3. Friedel–Crafts benzoylation of toluene

Benzoylation of aromatics is an important reaction in synthetic organic chemistry. It is unfortunate that many industries continue using the harmful halogen-containing Lewis acids such as $AlCl_3$ and BF_3 as catalysts to perform this reaction. The need to replace such catalysts with the more eco-friendly heterogeneous ones is felt all the more in recent years. In our work, we have found that these ferrospinel samples function as efficient heterogeneous catalysts for the liquid phase benzoylation of toluene.

The product yield was found to be proportional to the amount of the catalyst taken and to the duration of the reaction run. The catalyst samples remained

essentially insoluble in the reaction mixture, proving the heterogeneity of the process. We had optimised the conditions such that a reaction run for half an hour, employing 0.100 g of the catalyst each time, gave sufficient range in the yield of the products so that proper comparison of the catalytic activities of the various samples could be made. The reaction always yielded mainly two products, which were estimated by GC and identified as 2-methylbenzophenone (2-MBP) and 4-methylbenzophenone (4-MBP) by GC-MS. From the molar ratio of the reactants employed, it is calculated that a GC peak area percentage of 45.04 for the product corresponded to 100% yield in the reaction. Using this relation, the product yields were calculated from the primary GC data. The product yields were converted to intrinsic rate constants assuming a first-order situation.

3.3.1. Results

The product yield, rate constant and the selectivity of 4-MBP for the benzoylation of toluene are given in Table 4. From these data, the following conclusions can be drawn:

1. Cobalt ferrite is the most active catalyst at the lower activation temperature, while copper ferrite is the most active one at the higher activation temperature. In any case, nickel ferrite is the least active.
2. Sulphation does not influence much the catalytic activity at the activation temperature of 300°C, while it brings down the catalytic activity at the activation temperature of 500°C, compared to the activity of the unmodified samples.
3. Except for sulphated nickel ferrite, there is always an increase in the catalytic activity with increase in activation temperature.
4. The selectivity of 4-MBP remains more or less constant in the range 83–86%.

3.3.2. Discussion

Benzoylation of toluene has been reported over various heterogeneous catalysts such as calcined iron sulphate [34], sulphated zirconia [35], sulphated alumina [36], acidic zeolites [37], sulphated alumina–zirconia [38], a variety of sulphated metal oxides [39] and Si-MCM-41 supported gallium and indium [40]. Among these systems, all but the last mentioned are superacidic. The authors attribute the

Table 4

Benzoylation of toluene with benzoyl chloride over the ferrospinels of nickel, cobalt and copper[a]

Catalyst system	$T = 573$ K			$T = 773$ K		
	Product yield (%)	Rate constant (10^{-2} h^{-1} m^{-2})	Selectivity of 4-MBP	Product yield (%)	Rate constant (10^{-2} h^{-1} m^{-2})	Selectivity of 4-MBP
NiFe$_2$O$_4$	23.4	3.5	83.0	17.1	8.3	84.2
CoFe$_2$O$_4$	44.5	12.5	84.2	25.4	18.2	84.4
CuFe$_2$O$_4$	59.5	9.6	85.6	42.3	55.6	84.4
SO$_4^{2-}$/NiFe$_2$O$_4$	36.6	4.7	83.8	15.7	4.4	84.6
SO$_4^{2-}$/CoFe$_2$O$_4$	45.6	11.3	85.0	27.0	13.6	85.9
SO$_4^{2-}$/CuFe$_2$O$_4$	57.1	9.0	85.1	35.2	26.7	86.2

[a] T: activation temperature, toluene–benzoyl chloride molar ratio = 3.6:1, reaction temperature = 120°C, reaction time = 0.5 h, amount of catalyst = 0.1 g.

catalytic activity for acylation reaction to the superacidic Lewis or Bronsted sites. These ferrospinel samples are not expected to be superacidic as such, nor has such a quality been created by sulphation as evidenced by IR studies. n-Butylamine adsorption data (Table 3) show that there is a considerable increase in weak and medium strong acid sites as a result of sulphation for the catalysts activated at 300°C. But the benzoylation activity data (Table 4) show that sulphation does not affect the catalytic performance very much. Thus, we infer that weak and medium strong acid sites are not involved in benzoylation reaction. That leaves the strong acid sites, which are usually of the Lewis-type [33]. Aramendia et al. [41], using temperature-programmed desorption mass spectrometry (TPD-MS) techniques with pyridine, 2,6-dimethylpyridine and carbon dioxide as probe molecules, showed that the effect of calcination temperature on acidity of metal oxides surfaces was to reduce the number of Bronsted sites and to leave only the Lewis-type sites among the strongest acid sites. Thus, at the higher calcination temperature, most of the Bronsted acid sites would have disappeared and, at the same time, the strength and number of Lewis acid sites per unit surface area would have increased due to creation of surface defects and more coordinatively unsaturated cations. The catalytic activity for benzoylation increases with increase of activation temperature of the catalysts. Based on these observations, we come to the conclusion that the catalytic activity of the ferrospinel samples for benzoylation reaction is due to the strong Lewis acidic sites present in these systems.

In their study of liquid phase Friedel–Crafts benzylation of benzene over spinel-type copper chromium

ferrite samples, Ghorpade et al. [42] found that copper ferrite gave the highest yield of products; they concluded that the Lewis sites were responsible for the good catalytic performance. As sulphation delays dehydroxylation [17], the creation of strong and new Lewis acid sites on sulphated samples will be less efficient compared to the unmodified samples. This explains the smaller influence of activation temperature on the catalytic performance of the sulphated samples compared to the case with the unmodified systems.

The acidity of electron deficient defects on the metal oxide surface depends on the electronegativity of the metal cation [32,33]. As mentioned earlier, the electronegativities of the cations vary in the order: Fe^{3+} $\gg$ Cu^{2+} > Ni^{2+} $\cong$ Co^{2+}, as computed using Sanderson's procedure [29]. Evidently, the strong Lewis acidity of the ferrites originates primarily from the presence of tripositive ferric ions. Among the dipositive ions, Cu^{2+} provides the strongest Lewis acid sites. This may be due to its acquiring a stable, completely filled d-subshell on receiving an electron.

The rate of benzoylation depends both on the number and strength of the Lewis acid sites. The data in Table 3 show that cobalt ferrite has the largest number of strong acid sites. This correlates with the highest catalytic activity of cobalt ferrite for benzoylation at the activation temperature of 300°C. The higher activity of copper ferrite over nickel ferrite can be explained on the assumption that the benzoylation reaction requires the presence of strong Lewis acid sites of a certain minimum strength. The proportion of the Lewis acid sites above this minimum is higher in copper ferrite due to the higher electronegativity of Cu^{2+} ion over the Ni^{2+} ions. Thus, copper ferrite proves to
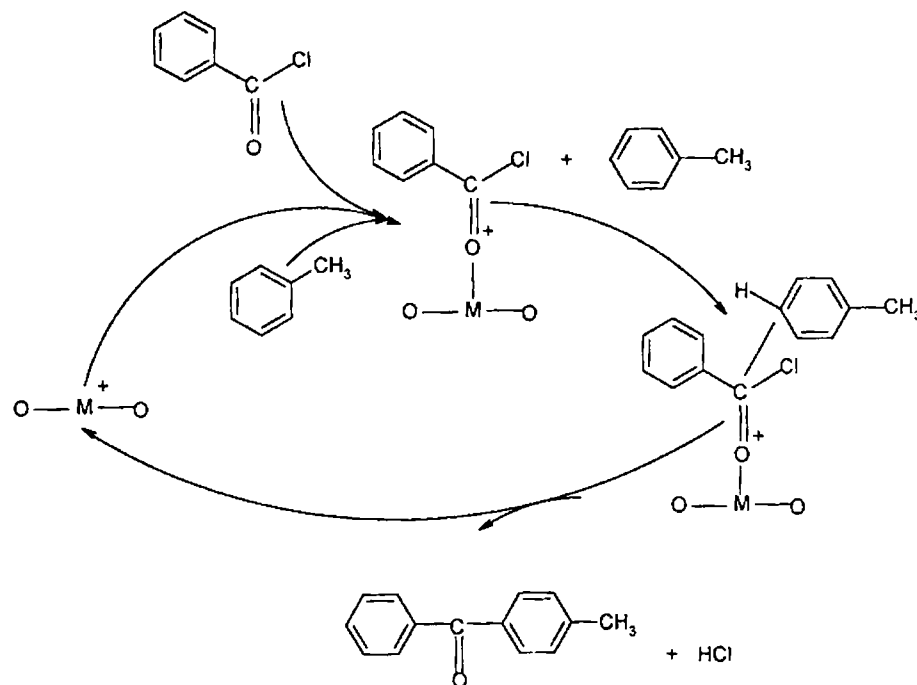
+ HCl

Fig. 7. A plausible mechanism for benzoylation of toluene by ferrospinel catalyst samples.

be a more active catalyst for the benzoylation reaction than nickel ferrite. Samples of copper ferrite activated at 500°C show the highest catalytic activity. This is due to the fact that copper ferrite is more vulnerable to the creation of anion vacancy defects on calcination than the other ferrites. The higher reducibility of copper ions [43], its special coordination described as (4 + 2) coordination [31] and the higher thermal instability of copper(II) oxide [30] are responsible for this susceptibility. Coupled with these, the drastic decrease in surface area with activation temperature results in very high surface density of Lewis acid sites of the proper strength on copper ferrite, making it the most active catalyst at the higher calcination temperature.

The mechanism of homogeneous Friedel–Crafts acylation is not completely understood, but at least two mechanisms are probably operative: one involving the acyl cation RCO^+ as the attacking species and the other involving a 1:1 complex formed between RCOCl and the Lewis acid catalyst, as the attacking species [44]. In many of the earlier studies [35,36,38] on the benzoylation of toluene by heterogeneous catalysts, it was reported that the reaction takes place

through the creation of benzoyl cation by the reaction of superacidic Bronsted acid sites of the catalysts with benzoyl chloride. But there is no evidence for superacidity in these ferrospinel systems. The effect of activation temperature and the effect of sulphation strongly suggests that, in the present case, the reaction involves the interaction of the Lewis acid sites of the catalyst with benzoyl chloride. As the reaction mixture has a net non-polar nature, a complex between the catalyst and benzoyl chloride is a more likely intermediate here than a free benzoyl cation. A plausible mechanism can be represented by Fig. 7. A comparison of the yields of the most active catalysts for the Friedel–Crafts reaction of toluene with benzoyl chloride reported by some of the earlier workers [34–39] with our results shows that these ferrospinel samples are indeed excellent catalysts for the said reaction.

4. Conclusion

Preparation of ferrospinels of nickel, cobalt and copper by low temperature coprecipitation method

produced homogeneous and fine particles with high surface areas. Sulphation studies on spinels are being reported for the first time. Sulphation caused an increase in the surface areas of most of the samples and delayed dehydroxylation of the samples on calcination. Sulphation also caused a tremendous increase in the number of weak and medium strong acid sites, while the strong acid sites were left unaffected.

Adsorption studies using electron acceptors of varying electron affinity values showed that copper ferrite has both the highest proportion of medium to strong basic sites and also the lowest proportion of weak basic sites. The basicity of all the ferrites reduced significantly on sulphation. The intrinsic catalytic activity for benzoylation of toluene with benzoyl chloride decreased among the transition metal ferrites in the order: cobalt > copper ≫ nickel at the activation temperature of 300°C and in the order: copper ≫ cobalt > nickel at the activation temperature of 500°C. Sulphation of the ferrites caused little change on their catalytic activity for the benzoylation of toluene. The effects of sulphation and catalyst activation temperature on the reaction rates for the benzoylation of toluene lead us to conclude that this reaction is catalysed by the strong Lewis acid sites provided by the octahedral cations on the spinel surface. The well-documented thermal instability of copper(II) oxide imparts some thermal instability in the copper ferrite too. Calcination of such samples creates more surface defects in terms of coordinatively unsaturated cations and trapped electrons. This is the cause of the simultaneous increase in the Lewis acidity and Lewis basicity in copper ferrite on calcination.

Acknowledgements

References

[1] C.M. Srivastava, in: B. Viswanathan, V.R.K. Murthy (Eds.), Ferrite Materials – Science and Technology, Springer, New Delhi, 1990, p. 85.

[2] J.P. Jacobs, A. Maltha, J.G.H. Reintjes, J. Drimal, V. Ponec, H.H. Brongersma, J. Catal. 147 (1994) 294.

[3] P.S. Anilkumar, J.J. Shrotri, S.D. Kulkarni, C.E. Deshpande, S.K. Date, Mater. Lett. 27 (1996) 293.

[4] K. Sreekumar, T.M. Jyothi, M.B. Talwar, B.P. Kiran, B.S. Rao, S. Sugunan, J. Mol. Catal. 152 (2000) 225.

[5] B.S. Rao, K. Sreekumar, T.M. Jyothi, Indian Patent 2707/98, (1998).

[6] K. Arata, Adv. Catal. 37 (1990) 165.

[7] J.C. Wu, C.S. Chung, C.I.. Ay, I. Wang, J. Catal. 87 (1984) 98.

[8] N.J. Jebarathinam, V. Krishnaswamy, in: P. Kanta Rao, B.S. Benwal (Eds.), Catalysis — Present and Future, Wiley, New Delhi, 1995, p. 288.

[9] A.I. Vogel, A Text Book of Practical Organic Chemistry, 3rd Edition, ELBS, London, 1973, p. 177.

[10] C. Whiston, in: F.E. Prichard (Ed.), X-ray Methods, Wiley, New York, 1991, p. 110.

[11] H. Lipson, H. Steeple, Interpretation of X-ray Powder Diffraction Patterns, Macmillan, London, 1970, p. 261.

[12] R.D. Waldron, Phys. Rev. 99 (1955) 1727.

[13] O. Saur, M. Bensitel, A.B.M. Saad, J.C. Lavalley, C.P. Tripp, B.A. Morrow, J. Catal. 99 (1986) 104.

[14] B.A. Morrow, R.A. McFarlane, M. Lion, J.C. Lavalley, J. Catal. 107 (1987) 232.

[15] M. Bensitel, O. Saur, J.C. Lavalley, B.A. Morrow, Mater. Chem. Phys. 19 (1988) 147.

[16] M. Waquif, J. Bachelier, O. Saur, J.C. Lavalley, J. Mol. Catal. 72 (1992) 127.

[17] X. Song, A. Sayari, Catal. Rev.-Sci. Eng. 38 (3) (1996) 329.

[18] J.R. Sohn, H.J. Jang, J. Mol. Catal. 64 (1991) 349.

[19] C. Miao, W. Hua, J. Chen, Z. Gao, Catal. Lett. 37 (1996) 187.

[20] C. Monterra, G. Cerrato, F. Pinna, M. Signoretto, G. Strukul, J. Catal. 149 (1994) 181.

[21] K. Nakamoto, Infrared and Raman Spectra of Inorganic and Coordination Compounds, 4th Edition, Wiley, New York, 1986, p. 249.

[22] E.V.A. Ebsworth, D.W.H. Rankin, S. Cradock, Structural Methods in Inorganic Chemistry, ELBS/Blackwell Scientific Publications, UK, 1987, p. 287.

[23] J.M. Daniels, A. Rosencwaig, Can. J. Phys. 48 (4) (1970) 381.

[24] J.W. Niemantsverdriet, W.N. Delgass, Topics Catal. 8 (1999) 133.

[25] K. Esumi, K. Meguro, J. Colloid Interface Sci. 66 (1978) 192.

[26] K. Meguro, K. Esumi, J. Adhesion Sci. Technol. 4 (5) (1990) 393.

[27] D. Cordischi, V. Indovina, J. Chem. Soc., Faraday Trans. 72 (10) (1976) 2341.

[28] R.D. Shannon, Acta. Cryst. A 32 (1976) 751.

[29] R.T. Sanderson, Chemical Periodicity, Reinhold, New York, 1960.

[30] J.L.G. Fierro, J.F. Garcia de la Branda, Catal. Rev.-Sci. Eng. 28 (2/3) (1986) 265.

[31] A.F. Wells, Structural Inorganic Chemistry, 4th Edition, ELBS, London, 1979, p. 890.

[32] A. Auroux, A. Gervasini, J. Phys. Chem. 94 (1990) 6371.

[33] J. Kijenski, A. Baiker, Catal. Today 5 (1989) 1.

[34] K. Arata, K. Yabe, I. Toyoshima, J. Catal. 44 (1976) 385.

[35] M. Hino, K. Arata, J. Chem. Soc., Chem. Commun. (1985) 112.

[36] K. Arata, M. Hino, Appl. Catal. 59 (1990) 197.

[37] A.P. Singh, D. Bhattacharya, S. Sharma, J. Mol. Catal. 102 (1995) 139.

[38] Y. Xia, W. Hua, Z. Gao, Catal. Lett. 55 (1998) 101.

[39] K. Arata, H. Nakamura, M. Shouji, Appl. Catal. 197 (2000) 213.

[40] V.R. Choudrary, S.K. Jana, B.P. Kiran, J. Catal. 192 (2000) 25.

[41] M.A. Aramendia, V. Borau, I.M. Garcia, C. Jimenez, A. Marinas, J.M. Marinas, A. Porras, F.J. Urbano, Appl. Catal. 184 (1999) 115.

[42] S.P. Ghorpade, V.S. Darshane, S.G. Dixit, Appl. Catal. 166 (1998) 135.

[43] P.W. Atkins, Physical Chemistry, 3rd Edition, ELBS, UK, 1987, p. 268.

[44] J. March, Advanced Organic Chemistry, 4th Edition, Wiley, New York, 1999, p. 541.